

RECEIVED

JAN 26 1996

OSTI

West Valley Support Program

Final Report

External Corrosion of Tanks 8D-1 and 8D-2

**D. B. Mackey
R. E. Westerman**

May 1995

**Prepared for West Valley Nuclear Services
under Contract DE-AC06-76RLO 1830
with the U.S. Department of Energy**

**Pacific Northwest National Laboratory
Operated for the U.S. Department of Energy
by Battelle Memorial Institute**



DISCLAIMER

This report was prepared as an account of work sponsored by an agency of the United States Government. Neither the United States Government nor any agency thereof, nor Battelle Memorial Institute, nor any of their employees, makes any warranty, express or implied, or assumes any legal liability or responsibility for the accuracy, completeness, or usefulness of any information, apparatus, product, or process disclosed, or represents that its use would not infringe privately owned rights. Reference herein to any specific commercial product, process, or service by trade name, trademark, manufacturer, or otherwise does not necessarily constitute or imply its endorsement, recommendation, or favoring by the United States Government or any agency thereof, or Battelle Memorial Institute. The views and opinions of authors expressed herein do not necessarily state or reflect those of the United States Government or any agency thereof.

PACIFIC NORTHWEST NATIONAL LABORATORY

operated by

BATTELLE

for the

UNITED STATES DEPARTMENT OF ENERGY

under Contract DE-AC06-76RLO 1830

Printed in the United States of America

**Available to DOE and DOE contractors from the
Office of Scientific and Technical Information, P.O. Box 62, Oak Ridge, TN 37831;
prices available from (615) 576-8401.**

**Available to the public from the National Technical Information Service,
U.S. Department of Commerce, 5285 Port Royal Rd., Springfield, VA 22161**



This document was printed on recycled paper.

WEST VALLEY SUPPORT PROGRAM

Final Report

EXTERNAL CORROSION OF TANKS 8D-1 and 8D-2

D.B. Mackey
R. E. Westerman

May 1995

Prepared for
West Valley Nuclear Services
West Valley, New York
under Contract DE-AC06-76RLO 1830
with the U.S. Department of Energy

Pacific Northwest National Laboratory
Richland, Washington 99352

MASTER

DISCLAIMER

Portions of this document may be illegible in electronic image products. Images are produced from the best available original document.

SUMMARY

Tanks 8D-1 and 8D-2 at the West Valley Nuclear Services (WVNS) site, West Valley, New York, rest on layers of perlite brick contained within steel pans. The pans tend to collect water, which can contact the tanks directly and which also can be "wicked" to the external surfaces of the tank through the perlite brick. The presence of air in the tank vault is conducive to the formation of oxygen concentration cells, which can promote localized corrosion of the carbon steel tank wall.

Pacific Northwest Laboratory conducted an experiment to estimate the extent to which the external surfaces of the tanks could have corroded in the 30 years since their construction. Specimens of carbon steel, similar to that used in the tank construction, were partially embedded in an upright position in particulate perlite in closed containers maintained at both $30 \pm 5^\circ\text{C}$ and $90 \pm 5^\circ\text{C}$. The water line in the containers was maintained at two levels: above the perlite level (high water level tests) and below the bottoms of the specimens (low water level tests). The water used in the tests was obtained from the pan of tank 8D-1. The containers were maintained in an aerated condition. Specimens were examined after 3-, 6-, 12-, 18-, 24-, and 30-month exposures.

The corrosion specimens showed a rate of general, or "uniform," attack of $<0.10 \text{ mm/yr}$ [$<4 \text{ mil/year (mpy)}$], consistent with that which would be expected of a structural grade of carbon steel exposed to air-equilibrated, nonaggressive ground water. The general corrosion rate showed a significant dependence on test temperature, with the higher rate being associated with the higher temperature.

More importantly, the corrosion specimens exhibited severe nonuniform attack, attributable to the oxygen concentration cells present around the particles of perlite in the low water level tests and in the vicinity of the air-water interface in the high water level tests. The rate of pit deepening of the deepest pits, $\sim 0.25 \text{ mm/yr}$ ($\sim 10 \text{ mpy}$), was similar for both the 30°C and the 90°C tests, and did not appear to diminish during the course of the 30 months of the test. In the 90°C tests, pits up to 1.8 mm (70 mils) deep were observed at 18-, 24-, and 30-month test durations. These deep pits suggest that a pit deepening rate of $>0.5 \text{ mm/yr}$ ($>20 \text{ mpy}$) is possible under the test conditions employed. Such a rate of pit deepening could obviously not have been maintained on the actual tank walls since tank construction of the tanks, or the tanks would have already been perforated. Eventually, corrosion products on the surfaces of the tanks would be expected to fill and cover the pits and the regions around the pits, and thereby inhibit to some extent the transport of reactants (H_2O and O_2) to the active corrosion sites. And, as noted, the very deep pits were associated with a 90°C test, rather than a test at actual tank temperature, which is intermediate between the two test temperatures used in the corrosion studies.

The pitting rates observed in the present tests are of concern, however. Because the diminution in the rate of pit-deepening with increasing test times is unknown, and because the corrosion rates on the inside of the tanks is not accurately known (especially in tank 8D-1), the thickness of remaining tank-wall steel cannot be estimated accurately. It is therefore recommended that consideration be given to displacing the O_2 in the tank-vault annulus with an inert gas, such as N_2 or Ar, or preventing water from entering the tank-vault annuli and contacting the tank surfaces.

The present test results do not include possible effects of micro-organisms or radiation, nor do they take into account corrosion occurring on the inside of the tank.

CONTENTS

SUMMARY	1
LIST OF FIGURES	3
LIST OF TABLES	4
1.0 INTRODUCTION	5
2.0 OBJECTIVES	5
3.0 EXPERIMENTAL APPROACH	6
4.0 MATERIALS	9
4.1 STEEL	9
4.2 WATER	10
4.3 PERLITE	11
5.0 RESULTS	11
6.0 CONCLUSIONS	13

LIST OF FIGURES

1	Method of Exposing Steel Specimens to Conditions Simulating Those at the External Tank Surfaces	6
2	Two of Four Reaction Vessels Used in Corrosion Tests	7
3	Typical Appearance of Specimens Upon Removal from the 30°C Low-Water-Level Test and the 30°C High-Water-Level Test, 30-Month Exposure	15
4	Typical Appearance of Specimens Upon Removal from the 90°C Low-Water-Level Test and the 90°C High-Water-Level Test, 30-Month Exposure	16
5	Typical Appearance of Cleaned Specimens After 30-Month Exposure, 30°C, Low-Water-Level Test	17
6	Typical Appearance of Cleaned Specimens After 30-Month Exposure, 30°C, High-Water-Level Test	18
7	Typical Appearance of Cleaned Specimens After 30-Month Exposure, 90°C, Low-Water-Level Test	19
8	Typical Appearance of Cleaned Specimens After 30-Month Exposure, 90°C, High-Water-Level Test	20
9	Appearance of Cleaned Components of Crevice Specimen W-28/P-28, 90°C, Low-Water-Level Test, 30-Month Exposure	21
10	General ("Uniform") Corrosion as a Function of Exposure Time	22
11	Average Pit Depth as a Function of Exposure Time	23
12	Maximum Pit Depth as a Function of Exposure Time	24
13	Pit Depth Measurements after 18-Month Exposure	25
14	Pit Depth Measurements after 24-Month Exposure	26
15	Pit Depth Measurements after 30-Month Exposure	27

LIST OF TABLES

1	Composition of Steel Plate and Welding Electrode, wt. %	9
2	Composition of Pan Water Used in Corrosion Tests and Composition of (Initially Pure) Water after Contacting Particulate Perlite	10
3	Typical Composition of Perlite	11
4	Average General ("Uniform") Corrosion of Specimens From All Tests	28
5	Average Pit Depth of Eight Deepest Pits on Each Specimen From All Tests	28
6	Deepest Pits Observed on Each Specimen, All Tests	29

1.0 INTRODUCTION

Tanks 8D-1 and 8D-2 are large [21 m (70 ft) diameter, 8.2 m (27 ft) high] underground nuclear waste storage tanks located at the West Valley Nuclear Services (WVNS) site in West Valley, New York. The tanks were constructed in 1964 from ASTM 201 Grade A carbon steel, and they were stress relieved in place after fabrication. The tanks rest on a layer of perlite bricks. The bricks consist of a mixture of portland cement and expanded perlite. The joints between the bricks were filled with loose expanded perlite after the bricks were put in place. The brick layer lies inside a steel pan. The brick layer is centered in the pan and bound by a steel band.

The pans tend to collect and retain water (condensation, rain water, ground water). The external surfaces of the tank bottoms are assumed to have been in a moist condition since construction. The situation appears to be the most severe in the case of tank 8D-1, in that the tank and vault sit at an angle, and the pan pump inlet is not located at the low point of the pan. It appears that the bottom of tank 8D-1 can be exposed to liquid water, perlite brick inundated with liquid water, and moist brick that "wicks" water from the water pool. The bottom of tank 8D-2 appears to be in a drier condition, with the possibility of moist brick contacting the bottom of the tank to some undefined extent. The WVNS staff have expressed concern that the external corrosion resulting from these moist, oxygenated conditions could be capable of significantly reducing the thickness of the tank walls.

At ordinary temperatures, oxygen and moisture are the necessary factors for the corrosion of iron or steel in neutral or near-neutral environments. Both must be present at the same time, because oxygen alone or water free of dissolved oxygen does not corrode iron to any practical extent. The corrosion rate is, in general, roughly proportional to the activity of oxygen present. In addition, oxygen can cause localization of attack through the formation of differential aeration cells. Such cells are formed whenever iron is in contact with aerated solution at one place and with oxygen-deficient solution elsewhere. The oxygen-deficient areas become anodes and, therefore, are corroded more actively. Differential aeration cells commonly account for localized corrosion (pitting) under rust layers on iron, or accelerated corrosion in open crevices, or corrosion near the water line of submerged steel structures, such as pilings. Presence of salts (especially chlorides) that contribute to the electrical conductivity of the water can accelerate the corrosion, as can increasing temperature.^(a) The conditions existing at the bottom surfaces of tanks 8D-1 and 8D-2 can easily be construed to constitute conditions that could lead to both general and localized corrosion of the tank steel, because oxygen (air), water, and crevice conditions are simultaneously present. To study the extent of corrosion expected, Pacific Northwest Laboratory^(b) conducted corrosion tests under tank-simulating test conditions, with specimen exposures of 3, 6, 12, 18, 24, and 30 months.

2.0 OBJECTIVES

The studies described in this final report are intended to provide corrosion rate data on representative mild steel specimens exposed to conditions simulating those existing in the vicinity of the tank-bottom external surfaces. The extent of corrosion observed in the long-term tests (extending to 30 months) will permit an assessment of the magnitude of the potential corrosion problem.^(c) It can then be determined whether external-surface corrosion mitigation (e.g., by excluding air or water from the tank-vault annuli) is necessary to preserve confidence in long-term tank integrity.

- (a) See, for example, the discussion of these topics in the Corrosion Handbook edited by H. H. Uhlig, John Wiley and Sons, New York, 1948, pp. 125-143.
- (b) Pacific Northwest Laboratory is operated by Battelle Memorial Institute for the U. S. Department of Energy (DOE) under Contract DE-AC06-76RLO 1830.
- (b) The results of the 3- and 6-month tests were presented in a progress report to WVNS entitled, "External Corrosion of Tanks 8D-1 and 8D-2," March 25, 1993; the results of the 12-month tests were presented in a report with the same title dated November 22, 1993.

3.0 EXPERIMENTAL APPROACH

The basic test approach involved simultaneously exposing mild steel specimens to (a) an environment of air, water, and water-immersed unexpanded perlite, and (b) an environment of air and moist unexpanded perlite. These two environments differ only in the position of the water table relative to the surface of the perlite. Each of the two environments described was being held at a temperature of $30 \pm 5^\circ\text{C}$ and $90 \pm 5^\circ\text{C}$, to span (conservatively) the temperature range of the two tank's operating histories. The two experimental conditions are shown schematically in Figure 1.

The water used in the tests was obtained from the pan underlying tank 8D-1. The water in the test vessels was changed every two weeks for the first 3 months of the test; the replacement frequency was then extended to a monthly schedule, which was maintained for the duration of the test. The perlite was not replaced during the course of the tests.

Each of the four reaction vessels contained 24 single specimens and two "crevice" specimens. The crevice specimens were simply two single specimens clamped tightly together. A flow of air was imposed on each test chamber to ensure the oxygen reactant did not become depleted during the tests. Typically, ~60 L of air was passed through the vessels each week, in three batches of ~20 L each, every other day. Each purge took ~10 min to complete. The reaction vessels were fitted with tight-fitting lids, and the tubing used for air conduction was fitted with condensers to minimize water loss.

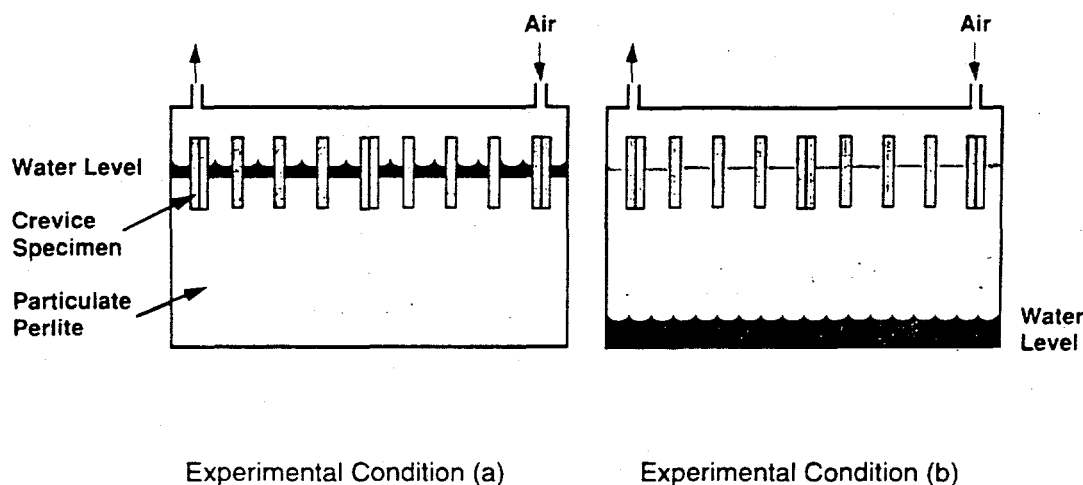


FIGURE 1. Method of Exposing Steel Specimens to Conditions Simulating Those at the External Tank Surfaces

Four reaction vessels, of the type shown in Figure 2, were used in the tests. The $30 \pm 5^\circ\text{C}$ tests used polyethylene containers, the $90 \pm 5^\circ\text{C}$ tests used stainless steel containers. (The water had not yet been added to the containers shown in Figure 2.) The crevice specimens, held together by clamps insulated with PTFE, can be seen in the specimen arrays. The specimens were inserted into the perlite to a depth of 64 mm (2.5 in.), which left 50 mm (2 in.) of specimen protruding above the perlite level. Pan water was added to the high-water-level tests until the level of water was 10 ± 5 mm (0.4 ± 0.2 in.) above the level of the perlite. Oxygen concentration cells were produced on specimens in this test; oxygen was reduced in the cathodic region of the cell at the air-water interface,

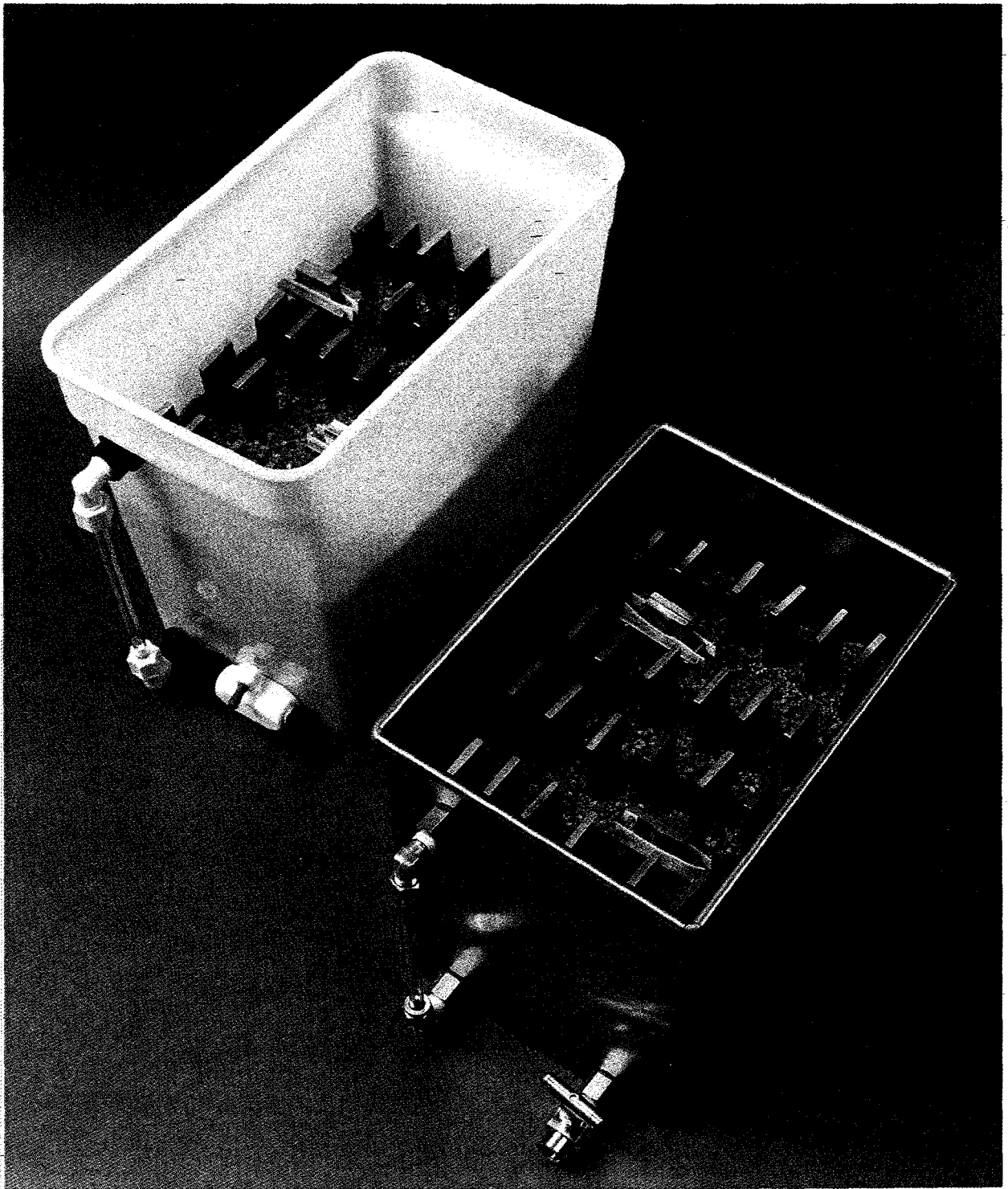


FIGURE 2. Two of Four Reaction Vessels Used in Corrosion Tests

and the anodic oxidation of iron took place in the vicinity of the air-water interface. Water was added to the low-water-level tests until the water level lay 100 ± 13 mm (4 ± 0.5 in.) below the level of the perlite [38 mm (1.5 in.) below the bottom of the steel specimens]. In these tests, water readily "wicked" through the perlite, and the surface of the perlite was observably moist. This moist perlite medium allowed both water and air to have access to the surface of the metal. Oxygen concentration cells would be expected to form at points of contact between the steel and the particles of perlite, producing pits in the anodic perlite-steel contact regions where oxygen was excluded.

At the conclusion of each test period, a fraction of the total number of test specimens were removed, cleaned, and examined for (a) general corrosion, by gravimetric methods, and (b) nonuniform corrosion, by optical methods. The data were analyzed to provide a rate-of-metal-loss for the WVNS tanks for both uniform corrosion and nonuniform corrosion modes, and these rates were then compared with the tank wall thickness.

The optical-micrometer procedure used for measuring the pit depths in the present study is summarized below:

- The optical micrometer was made by Edwards Aerospace Incorporated, Ontario, California (Model 966A, Serial No. 2812). The micrometer has an intrinsic accuracy of ± 0.0025 mm (± 0.0001 in.). It was supplied with two eyepieces, 15X and 20X, and two objective lenses, 5/.20 and 10/.25. The micrometer can be mounted on a tripod, permitting it to straddle the specimen to be examined. The operating surface was a machined metal flat, which permitted the micrometer to be moved over the surface of the specimen with a minimum of vertical-plane error. Some sliding was necessary, to enable a pit bottom to be referenced to relatively undisturbed original specimen surface.
- The eight deepest pits on each specimen were measured for the pit-depth quantification. The deepest pits were determined by means of oblique illumination of each side of each specimen with a small intense-beam flashlight. The deepest pits were marked and located on a "map" of each specimen. The map permitted rechecking of individual pits in case of inconsistencies in the data, and prevented recounts of the same pit if it was deemed necessary to increase the pit-count data base.
- The following guidelines were adopted in selecting pits for measurement:
 - The pits were not to be associated with a specimen edge or corner, without an intervening "ridge."
 - An individual pit was to be separated from other pits by a significant distance or by a well defined ridge.
 - The depths of individual pits should be referenced to undisturbed surface, where possible.
 - The micrometer screw eyepiece was to be used in one direction only for each pit measurement, to minimize screw "backlash."
 - The pits could be located on either side of the specimen, and there was no restriction on pit "diameter" (major dimension in the plane of the specimen surface).
- Testing of the micrometer technique on a number of pits with three operators revealed the best combination of lenses (15X eyepiece, 10/.25 objective), which balanced the requirements of area of field (low magnification) with minimum depth of focus (high magnification). Also, it showed that the "principal operator" (S. Faber) obtained the same results as the other two

pit measurement operation.

It is estimated that the depth of relatively shallow pits, i.e., those less than 0.25 mm (10 mils) deep, was determined with an accuracy of about $\pm 10\%$. Deeper pits are, in general, associated with a rougher background surface, with attendant difficulties in obtaining a clearly defined "benchmark" reference surface near the pit being measured. It is therefore estimated that the depth of pits in the range 0.25 to 1.0 mm (10 to 40 mils) can generally be measured with confidence to an accuracy of ± 0.05 mm (± 2 mils).

The corrosion tests were initiated in August 1992. Test durations of 3, 6, 12, and 24 months were originally planned. It was later decided, in consultation with WVNS staff, that the tests should be extended to 30 months, and that a portion of the remaining specimens should be removed from the test for examination at 18 months as well as at 30 months. This report summarizes and compares the corrosion data for all of the test durations; however, only photographs of the 30-month test specimens are included.

4.0 MATERIALS

4.1 STEEL

The steel specimens were made from one lot of plate material conforming to ASTM A-516 Grade 60 steel.^(a) Specimens of both unwelded plate and welded plate were included in the test. The welded specimens were welded with AWS E7018 electrode material, using the shielded-arc welding method. The compositions of the plate and electrode material are given in Table 1.

TABLE 1. Composition of Steel Plate and Welding Electrode, wt%

<u>Element</u>	<u>Plate</u>	<u>Electrode</u>
C	0.21	(a)
Cr	0.03	0.20 max
Cu	0.03	(b)
Mn	1.14	1.60 max
Mo	0.01	0.30 max
Ni	0.01	0.30 max
P	0.016	(b)
S	0.018	(b)
Si	0.23	0.75
V	(b)	0.08 max

(a) Not reported. Typically 0.04 to 0.07 wt% for this material.

(b) Not reported.

- (a) Specimens made of ASTM A-516 Grade 55 steel plate were ordered from the specimen vendor (Metal Samples Company, Munford, Alabama); specimens of ASTM A-516 Grade 60 steel were actually supplied. The Grade 60 material supplied is slightly higher in C (0.03%) and Mn (0.24%) than permitted by the Grade 55 specifications. The Grade 60 material was retained for the experimental work, because it was judged that the difference in composition would not significantly affect the corrosion test results.

The final specimen dimensions were 114 mm x 30 mm x 5.3 ±0.5 mm (4.50 in. x 1.20 in. x 0.21 ±0.02 in.). The weldment specimens were machined to their final thickness by milling the welded plate from the root side of the weldment. All the specimens were heat treated at 593°C in air for 1 h with a furnace cool before the final surface finishing to simulate the effect of the stress relief anneal of the waste tanks. For the final surface preparation, the bead side of each welded specimens was sand blasted, and the root side and edges were surface ground with 120-grit emery. All surfaces of the unwelded plate specimens were surface ground with 120-grit emery.

4.2 WATER

The water used in the tests was obtained from the pan of WVNS tank 8D-1. The water was shipped to PNL from WVNS in three 114-L (30-gal) plastic barrels. The water from the three barrels was blended at PNL to ensure that the source water would not vary significantly in composition during the corrosion study. An aliquot of the blended water was then taken for analysis. The composition of the water is given in Table 2. Also presented in the table is the composition of a distilled water "wash" that was allowed to contact an (approximately) equal volume of granular perlite that was obtained from the same source as the perlite placed in the test vessels. The perlite wash water has a much lower ion strength than the pan water, indicating that the perlite will not contribute significant impurities to the test medium. Additionally, all the perlite used in the tests was thoroughly rinsed in pan water, then drained, before being placed in the test vessels.

TABLE 2. Composition of Pan Water Used in Corrosion Tests and Composition of (Initially Pure) Water After Contacting Particulate Perlite

Chemical Specie	Concentration, mg/L	
	Pan Water	Wash Water
Al	0.04	0.19
Ca	8.4	0.36
Fe	--	0.1
K	115	--
Mg	2.8	--
Na	99	6.3
Si	31.5	2.0
B	0.1	0.05
F ⁻	--	2.8
Cl ⁻	10.7	0.45
NO ₃ ⁻	3.26	<0.1
SO ₄ ⁻⁻	206	3.35
Total carbon	34.4	1.94
Inorganic carbon	32.3	0.98
Total organic carbon	2.1	0.96
pH	9.8	8.4
Conductivity (µmho)	925	36.9

4.3 PERLITE

Perlite is a glassy volcanic rock that can be converted to a frothy material of low bulk density by rapidly heating the raw particulate material to a temperature of ~800°C. The constituents of perlite mined in the U.S. typically lie in the composition ranges given in Table 3. The perlite used in the present investigation is assumed to fall within the composition limits shown.

TABLE 3. Typical Composition of Perlite, wt% (a)

SiO ₂	72-75
Al ₂ O ₃	12-14
Na ₂ O	3-4
K ₂ O	4-5
CaO	0.5-1
Fe (total)	0.5-1
H ₂ O	3-5

When mixed with portland cement, expanded (or "popped") perlite forms a concrete with up to 20 times more thermal insulation than conventional concrete. The bricks underlying tanks 8D-1 and 8D-2 are composed of this insulating concrete material.

New perlite brick was not considered an option for the solid phase in the test vessels, either in slab or particulate form, because the alkaline constituents of the unleached, fresh brick surface would tend to reduce the corrosiveness of the environment and make the test results nonconservative. In the actual waste tanks, the perlite brick has been leached by ground water for a long period of time, and the alkalinity of the leachate would be expected to have decreased considerably. (This conclusion is consistent with the intermediate pH of the pan water, Table 2.) Plain particulate perlite was, therefore, selected as the matrix material for the test vessels. Initial trials were run with particulate expanded perlite, but its strong tendency to float was inconsistent with the object of a high waterline in experimental approach (a), Figure 1. Only a small fraction of the the material could be made to sink to the bottom of the test vessel, even using a vacuum impregnation approach. Recourse was made to unexpanded perlite, with a particle size (major dimension) of 2 to 4 mm. (b) Solid perlite material has a density of ~2.5 g/cm³ and the consistency, in particulate form, of very coarse sand. The mechanical properties of the particulate material are such that it is able to hold the embedded specimens firmly in place without ancillary supporting devices.

5.0 RESULTS

At the conclusion of each of the first three test periods (3, 6, and 12 months), one-fourth (24) of the original total of 96 single specimens was removed from the test vessels for examination. The 24-specimen total comprised 6 specimens from each test vessel, 3 unwelded and 3 welded. Of these, 2 of 3 were stripped of their corrosion product in inhibited 50% HCl solution for analysis of general and pitting corrosion, while the third specimen was archived in a desiccator. At the conclusion of each of the last three test periods (18, 24, and 30 months), 2 single specimens were removed from each vessel, 1 unwelded and 1 welded, for examination. None was archived.

(a) C. W. Chesterman. 1975. Industrial Minerals and Rocks, Edited by S. J. Lefond, 4th Edition, pp. 927-934.

(b) Obtained from Celite Corporation, P.O. Box 519, Lompoc, CA 93438-0519.

At the end of the 30-month test all of the crevice "pair" specimens (8 pairs total) were examined

At the end of the 30-month test all of the crevice "pair" specimens (8 pairs total) were examined along with the remaining "single" specimens.

When the specimens were removed from the perlite, they were typically covered with a mass of corrosion product (typical hydrated iron oxides, or "rust") with embedded perlite particles. The appearance of the specimens after the 30-month test period is shown in Figures 3 and 4. The crevice specimens were arbitrarily selected for these figures--the "single" coupons displayed a similar appearance.

The appearance of the specimens after corrosion product removal in inhibited HCl solution is shown in Figures 5 through 9. The relatively aggressive nonuniform attack is evident from the figures. It is also evident that the higher temperature produced a significantly greater degree of attack. It was noted earlier (progress report, PNL to WVNS, November 22, 1993) that significant attack occurred in what would ordinarily be considered the "vapor phase" region of the test specimen. This phenomenon was again observed, e.g., Figure 7 in this report. Water apparently migrated up the coupon via the corrosion product layer, and would be expected to become enriched in electrolytes through evaporation. The phenomenon produced pits of significant depths, possibly because of the ready availability of oxygen and a relatively high ionic strength electrolyte.

The internal surfaces of the crevice coupons showed very little attack, in all cases, compared to the external surfaces. The appearance of a typical crevice specimen is shown in Figure 9. In the case of the welded specimens, no unusual corrosion attack appeared to be associated with any of the features of the weldment (e.g., bead or heat-affected zone).

The quantification of the general ("uniform") corrosion attack by gravimetric methods is shown in Figure 10. Data for all the test exposures are included in the figure. In using gravimetric data to compute the average, or "uniform," penetration results from the test coupons, it was assumed throughout the study that only the immersed or embedded area of the single coupons would be considered the affected area in the metal penetration computation, and that only the outside regions of the crevice coupons, immersed or embedded, would be considered the affected area in the penetration computation. Such assumptions cause computational errors in the "conservative" direction. That is, the calculated corrosion rates will be somewhat higher than the actual rates for coupons undergoing significant corrosion outside of the areas defined, including coupons undergoing corrosion in the "vapor phase" region.

There is a great deal of scatter in the data presented in Figure 10, at least partially because each data point after 12 months is the result of the analysis of only one specimen. The curves appear to exhibit a definite "leveling off" tendency with increasing time, but the data are not of long enough duration and the data scatter is too great to attempt a quantification of the rate diminution versus test time.

The effect of temperature is obvious on the general corrosion observed; no other variable, i.e., welded versus unwelded or water level had a significant effect on the overall test results. The range of general corrosion rates shown in the figure is not significant from the standpoint of tank integrity, as an extrapolation of the slopes of the curves would result in a long-term maximum corrosion rate of only <0.10 mm/yr (<4 mpy).

The uniform corrosion, however, is not the principal concern to the integrity of tanks 8D-1 and 8D-2; nonuniform corrosion, such as that associated with pitting (on a small scale) or an oxygen concentration cell acting at a water-air interface (on a large scale) is of more concern. The average and maximum pit-depth results for all of the test exposures are shown in Figures 11 and 12, respectively. The individual data points for the 18-, 24-, and 30-month tests are shown in Figures 13 through 15. The data used to generate the figures are tabulated in Tables 4, 5, and 6.

Though in any given structure the deepest pit is potentially the most important, the data of Figure 11 are intended to show whether a general diminution in rate is observed with time. The data of Figure 12 are intended to show the severity of the observed pitting, and whether the rate of deepening of the most advanced pits tends to slow with time. The data plots of Figures 13 through 15 are intended to display the range of pit depths observed in the longest duration tests, the changes in the pit-depth distribution with time, the potential effects of welded versus nonwelded regions of the tank walls, and to call out the appearance of pits in "unexpected" regions of the test specimens (such as the region in the vapor phase).

The rate of increase of pit depth (Figure 11) shows a definite decrease with time of exposure. The curves are essentially "flat" between 12 months and 30 months. A different picture emerges, however, when the maximum pit depth is plotted as a function of test time (Figure 12). This plot shows a pit-deepening rate (of the deepest pits) of ~0.25 mm/yr (~10 mpy), both for the 30°C tests and the 90°C tests, with unusually deep "vapor phase" pits observed in the 90°C tests (Figures 13, 14, 15). These very deep pits are associated with pit-deepening rates >0.5 mm/yr (>20 mpy), at the longest term (30-month) test duration.

Such a rate of pit deepening could not have been maintained on the actual tank walls [<13 mm (<0.5 in.) thick in some regions, as-built] since construction, or they would have already been perforated. Apparently, corrosion products on the tank surface eventually covered the pits and the regions around the pits, and thereby inhibited to some (unknown) extent the transport of reactants (H_2O and O_2) to the active corrosion sites. This diminution of pit-deepening rate with time is known and expected. The pit-deepening rate of the deepest pits observed in the present tests is reason for concern, however. Because it is not known when the rate would be expected to decrease, and because the overall penetration that has occurred from the inside of the tanks is not precisely known, the thickness of remaining steel in the tank wall cannot be estimated accurately from the present data. Also, the varied conditions existing around the tank, coupled with material and fabrication singularities associated with large-system construction, would be expected to produce some regions of the tank having unusual vulnerability to corrosion, compared to the present tests. Because the principal corrosion attack occurs because of the simultaneous presence of O_2 and H_2O in the tank/vault annulus, the corrosion could be greatly inhibited by eliminating the O_2 . Complete elimination of water, considered to be more difficult, would stop the corrosion entirely.

6.0 CONCLUSIONS

The corrosion specimens show a rate of general ("uniform") attack that does not pose a significant risk to tank integrity. The general rate is consistent with that expected of structural grade carbon steel exposed to air-equilibrated ground water, given the temperatures involved and the nonaggressive ground water employed in the corrosion tests. Only the test temperature significantly affected the rate of general corrosion--regardless of water level or whether the specimen contained a weldment.

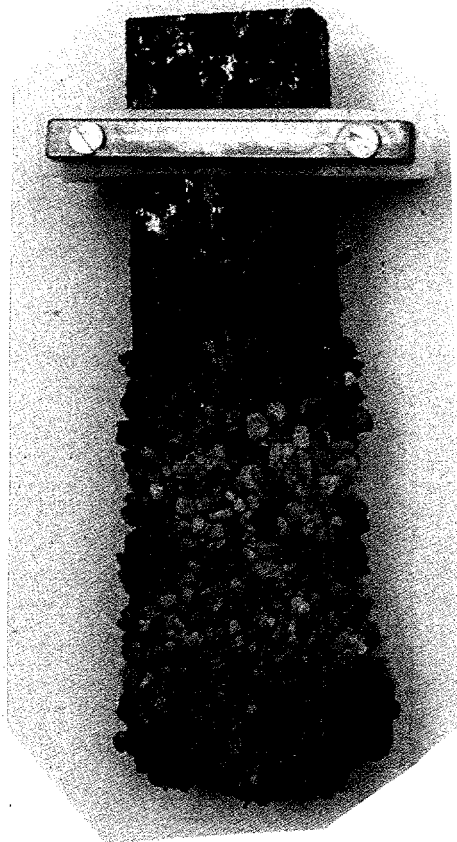
In the crevice specimens, no unusual corrosion was found within the crevices or on the specimen edges adjacent to the crevice openings. The internal crevice surfaces exhibited far less corrosion than the external surfaces of the crevice corrosion.

The nonuniform corrosion presents a cause for concern, because the pit-deepening rates are high and are not obviously decreasing with time in the case of the deepest pits. The temperature had the only significant effect on the pit-deepening rate, with the 90°C test producing very deep pits in the vapor-phase region of certain test coupons. However, the general trend of maximum pit depth for both 30°C and 90°C tests of about 0.25 mm/yr (10 mpy), or 7.5 mm (0.3 in.) in 30 years,

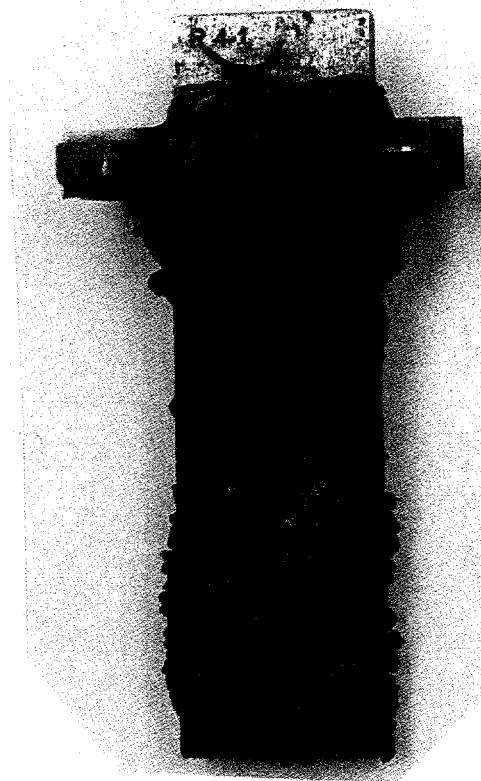
is uncomfortably high, when it is considered that the tank wall is <13 mm (<0.5 in.) thick in some regions, and that the present corrosion study deals with external tank corrosion only.

It is suggested that WVNS either investigate means to eliminate the water from the annulus of tanks 8D-1 and 8D-2, or displace the O₂ from the annuli with an inert gas.

The present test results do not include possible effects of micro-organisms or radiation, nor do they take into account corrosion occurring on the inside of the tank.

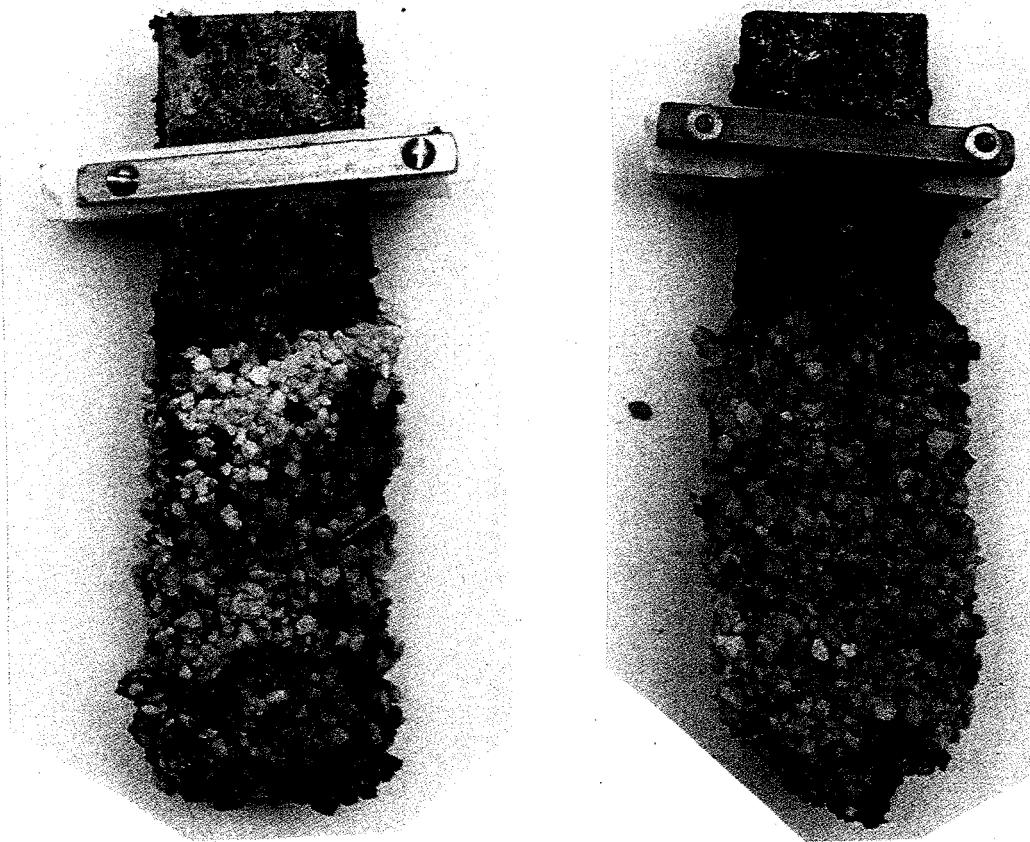


W-55/P-55



W-41/P-41

FIGURE 3. Typical Appearance of Specimens Upon Removal from the 30°C Low-Water-Level Test (left) and the 30°C High-Water-Level Test (right), 30-Month Exposure. Specimens shown are crevice-type specimens before disassembly. They are encrusted with corrosion product and embedded perlite particles. Specimens are shown approximately 90% actual size.



W-28/P-28

W-14/P-14

FIGURE 4. Typical Appearance of Specimens Upon Removal from the 90°C Low-Water-Level Test (left) and the 90°C High-Water-Level Test (right), 30-Month Exposure. Specimens shown are crevice-type specimens before disassembly. They are encrusted with corrosion product and embedded perlite particles. Specimens are shown approximately 90% actual size.

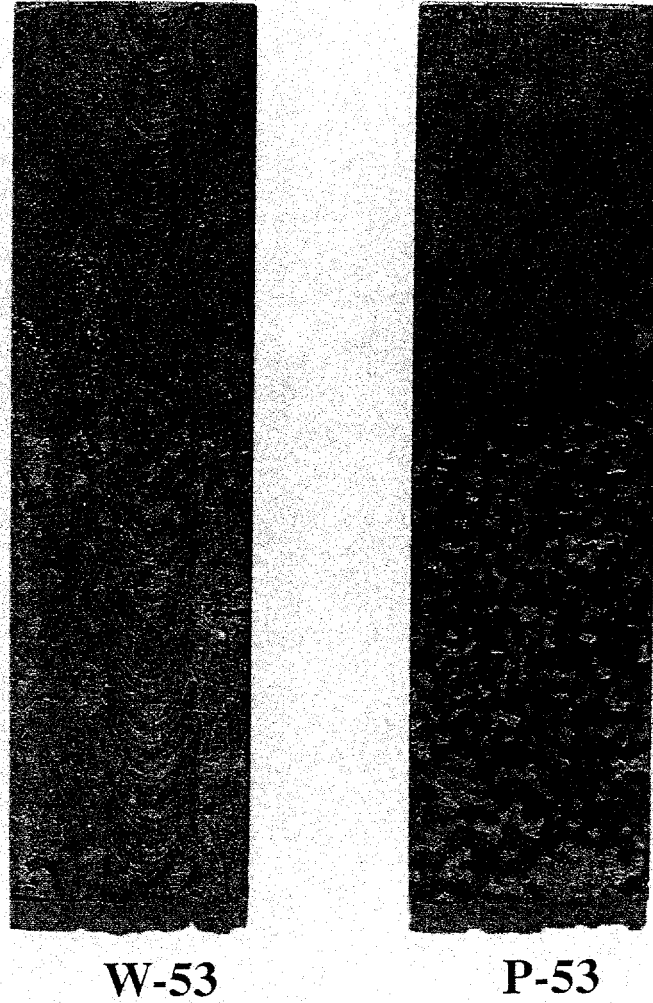
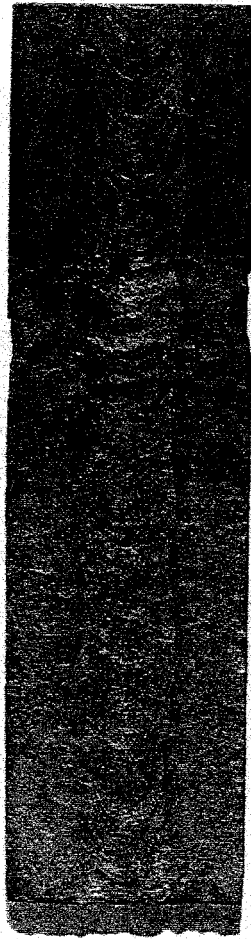


FIGURE 5. Typical Appearance of Cleaned Specimens After 30-Month Exposure, 30°C, Low-Water-Level Test. Specimens shown approximately actual size.

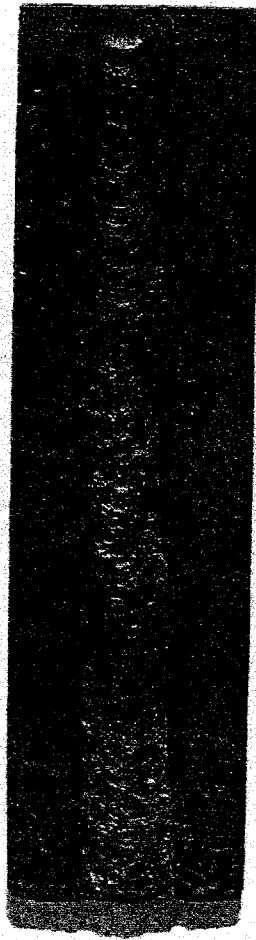


W-39



P-39

FIGURE 6. Typical Appearance of Cleaned Specimens After 30-Month Exposure, 30°C, High-Water-Level Test. Specimens shown approximately actual size.



W-25



P-25

FIGURE 7. Typical Appearance of Cleaned Specimens After 30-Month Exposure, 90°C, Low-Water-Level Test. Specimens shown approximately actual size.

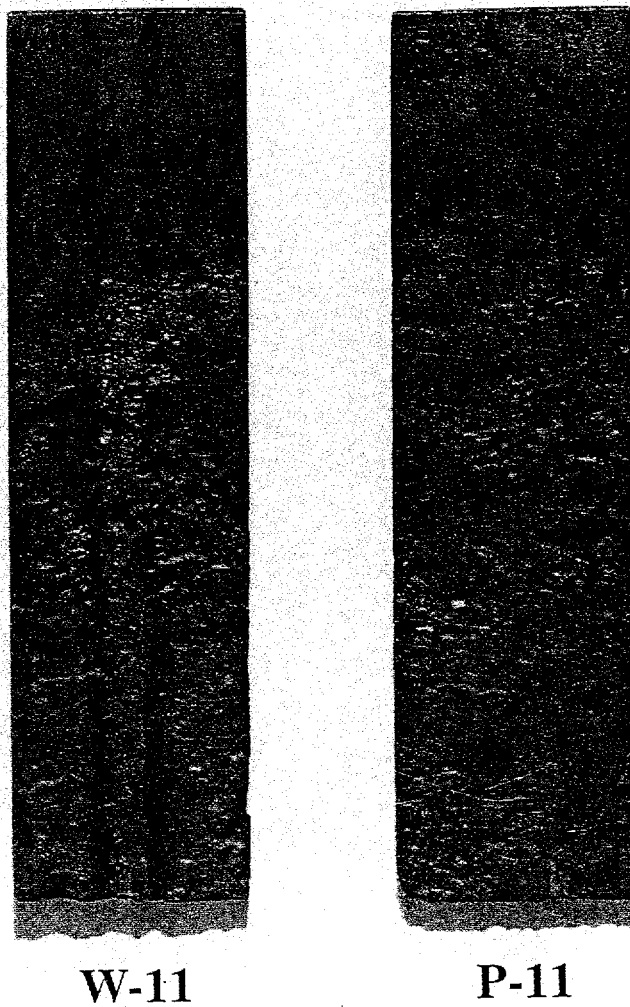


FIGURE 8. Typical Appearance of Cleaned Specimens After 30-Month Exposure, 90°C, High-Water-Level Test. The root side of the weldment of Specimen W-11 is shown in the figure. Specimens shown approximately actual size.

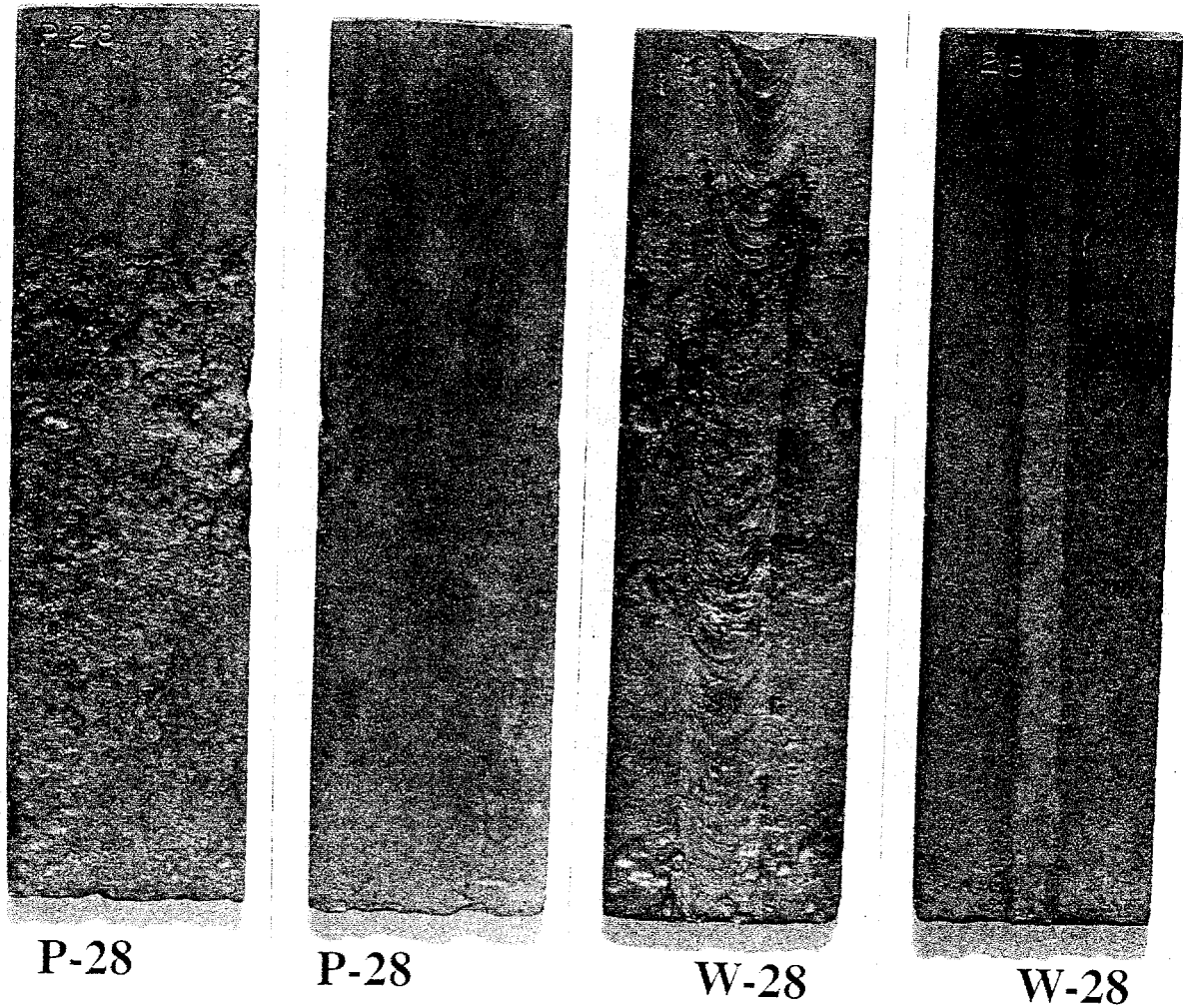


FIGURE 9. Appearance of Cleaned Components of Crevice Specimen W-28/P-28, 90°C, Low-Water-Level Test, 30-Month Exposure. The severely corroded surfaces (P-28, left; W-28, left) were the external surfaces of the crevice specimens. The internal surfaces exhibited much less corrosion attack than the external surfaces, and there was no evidence of true crevice corrosion. Specimens shown approximately actual size.

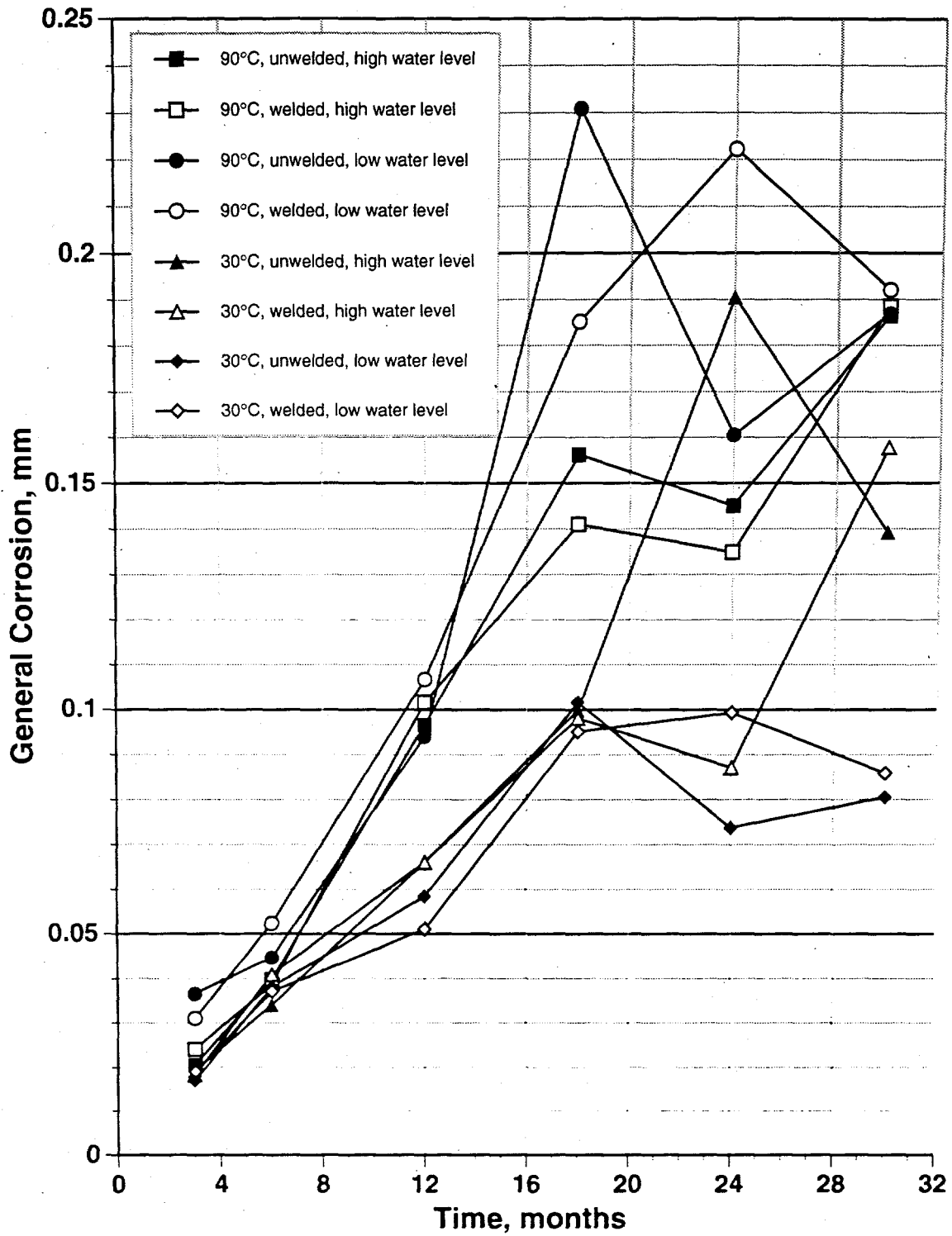


FIGURE 10. General ("Uniform") Corrosion as a Function of Exposure Time

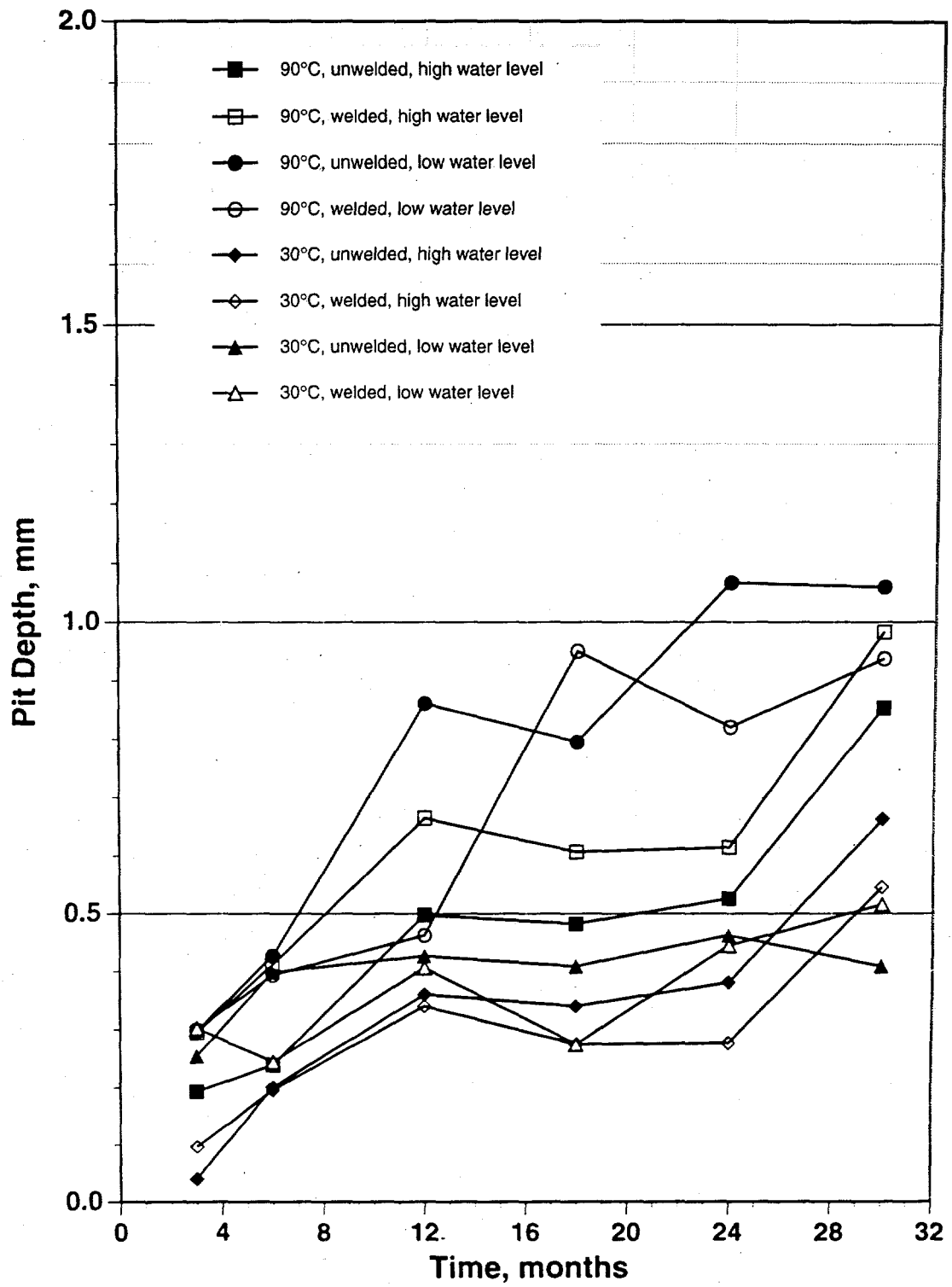


FIGURE 11. Average Pit Depth as a Function of Exposure Time

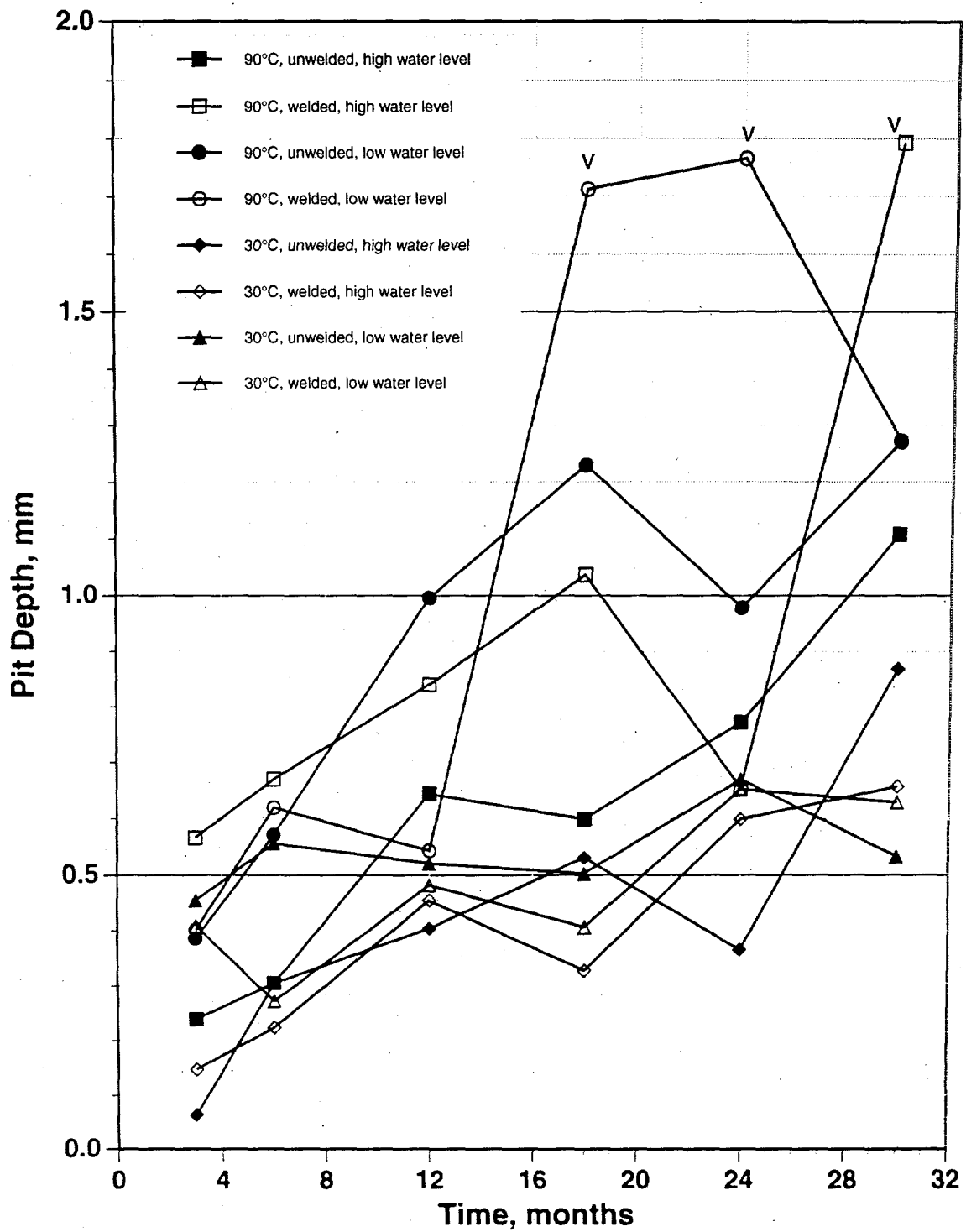


FIGURE 12. Maximum Pit Depth as a Function of Exposure Time. The three deepest pits (~1.8 mm deep) formed in the "vapor-phase" region of the test specimens; they are labeled with a "V" in the figure.

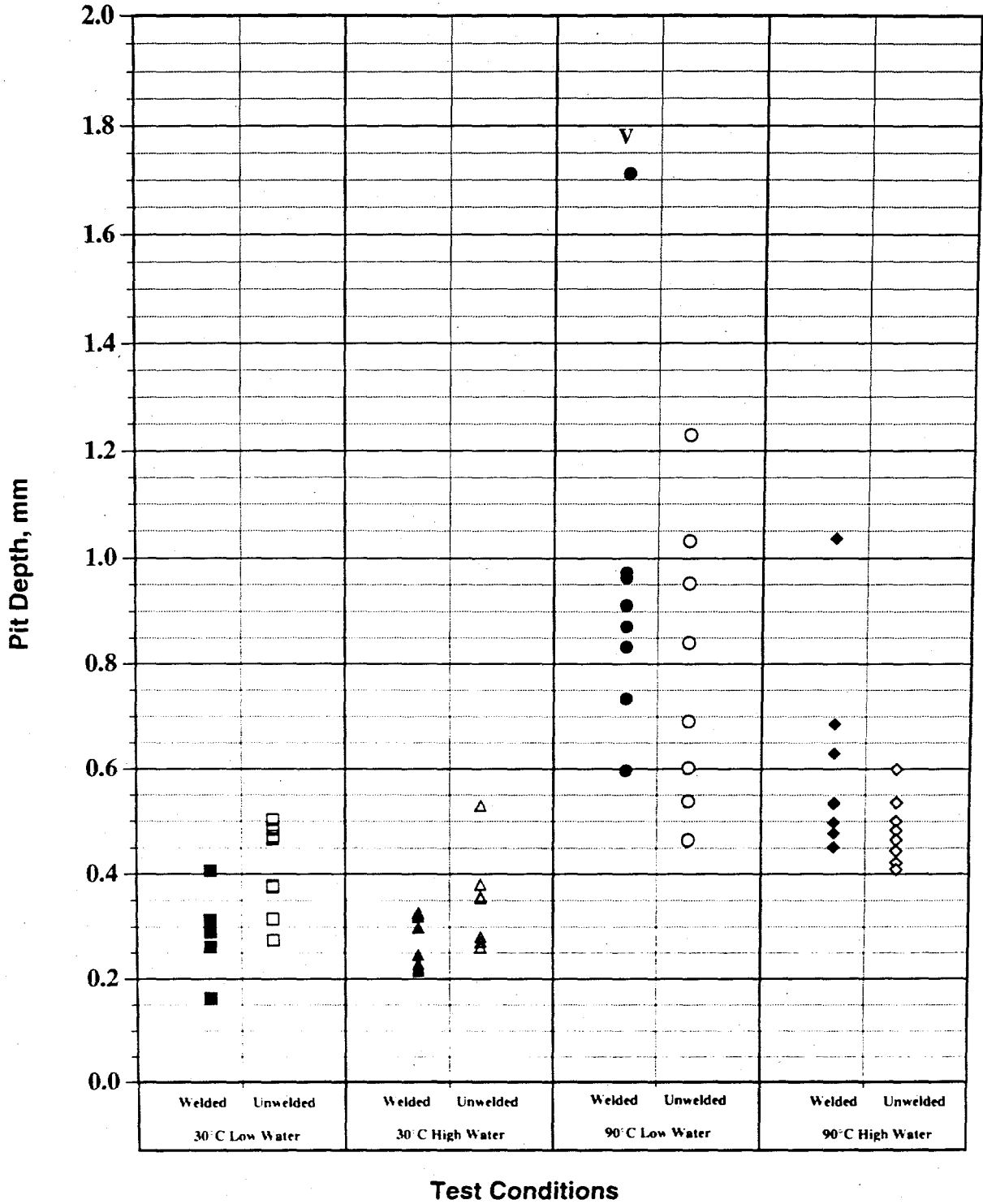


FIGURE 13. Pit Depth Measurements After 18-Month Exposure.
 V = "vapor phase" region of specimen.

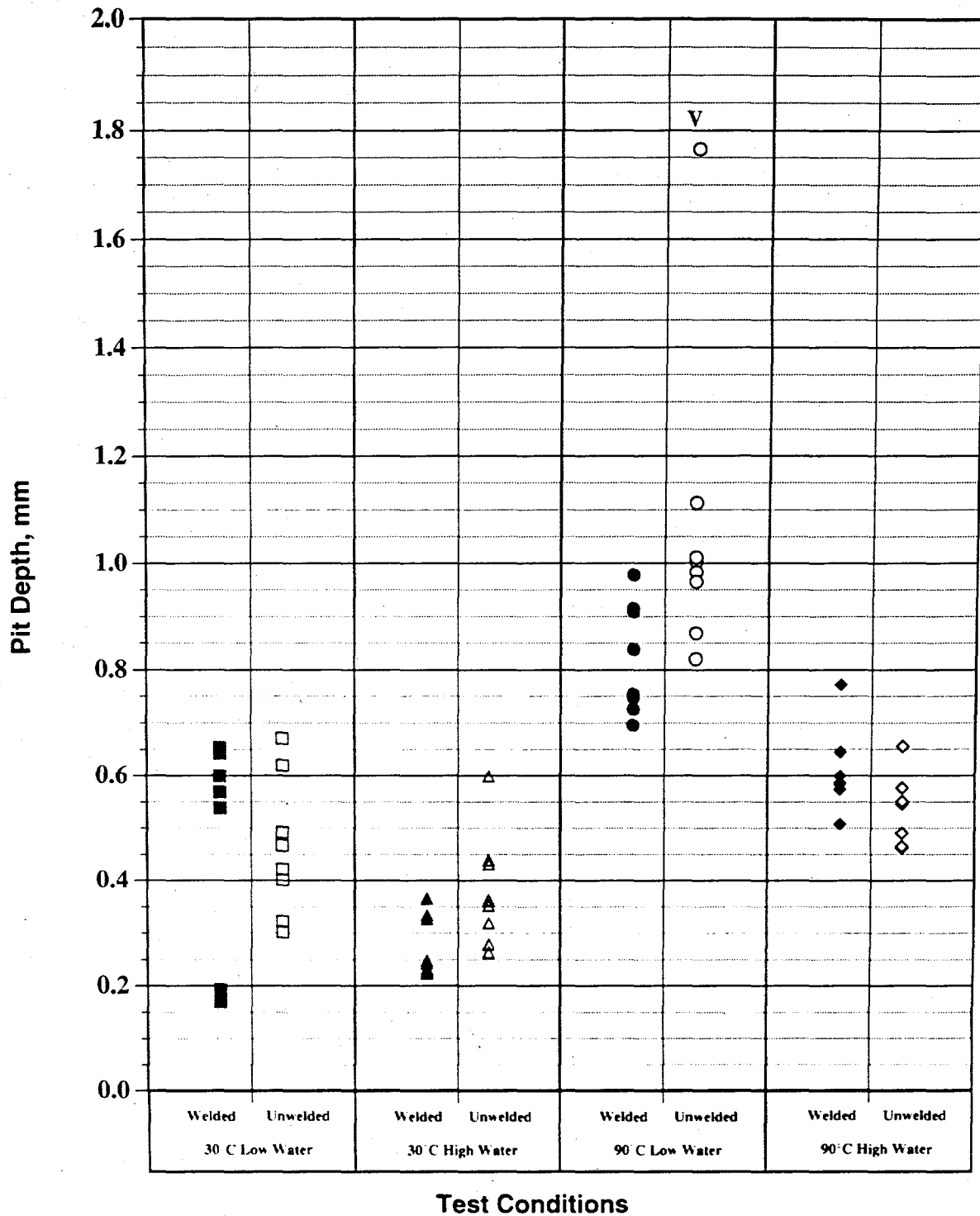


FIGURE 14. Pit Depth Measurements After 24-Month Exposure.
 V = "vapor phase" region of specimen.

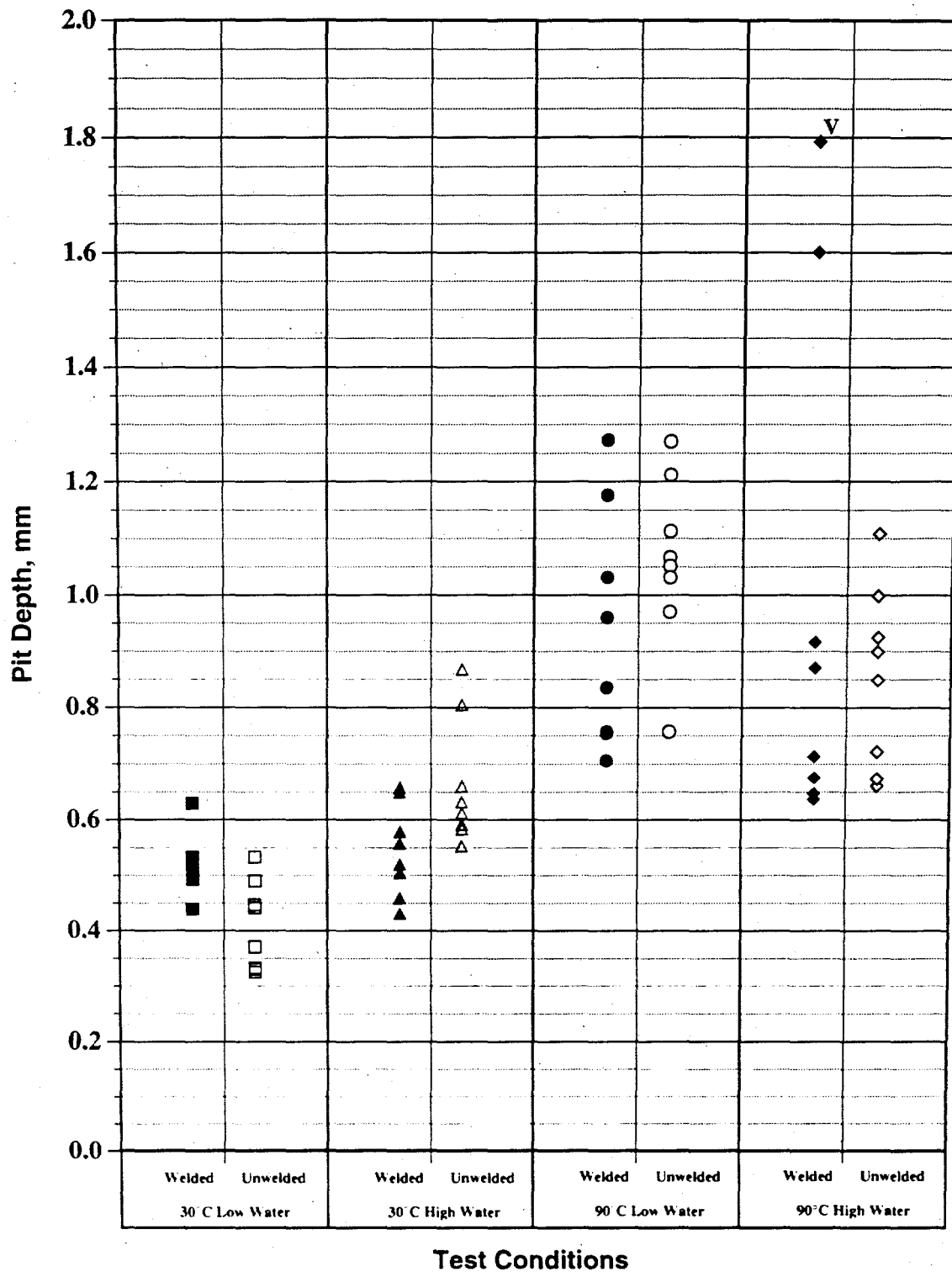


FIGURE 15. Pit Depth Measurements After 30-Month Exposure.
 V = "vapor phase" region of specimen.

TABLE 4. Average General ("Uniform") Corrosion of Specimens from All Tests, mm

Exposure, months	30°C, Welded Low water level	30°C, Unwelded Low water level	30°C, Welded High water level	30°C, Unwelded High water level	90°C, Welded, Low water level	90°C, Unwelded Low water level	90°C, Welded High water level	90°C, Unwelded High water level
3	0.019	0.017	0.018	0.019	0.031	0.037	0.024	0.021
6	0.037	0.038	0.041	0.034	0.052	0.045	0.039	0.040
12	0.051	0.058	0.069	0.066	0.107	0.094	0.102	0.097
18	0.095	0.102	0.098	0.100	0.185	0.231	0.141	0.156
24	0.099	0.074	0.087	0.191	0.222	0.161	0.135	0.145
30	0.086	0.081	0.158	0.139	0.192	0.187	0.188	0.186

TABLE 5. Average Pit Depth of Eight Deepest Pits on Each Specimen from All Tests, mm

Exposure, months	30°C, Welded Low water level	30°C, Unwelded Low water level	30°C, Welded, High water level	30°C, Unwelded High water level	90°C, Welded, Low water level	90°C, Unwelded Low water level	90°C, Welded High water level	90°C, Unwelded High water level
3	0.302	0.254	0.097	0.041	0.300	0.297	0.295	0.193
6	0.244	0.399	0.196	0.201	0.394	0.427	0.411	0.239
12	0.406	0.427	0.340	0.361	0.462	0.861	0.665	0.498
18	0.274	0.409	0.274	0.340	0.950	0.795	0.607	0.483
24	0.445	0.462	0.277	0.381	0.820	1.067	0.615	0.526
30	0.516	0.409	0.546	0.663	0.937	1.059	0.983	0.853

TABLE 6. Deepest Pits Observed on Each Specimen, All Tests, mm

Exposure, months	30°C, Welded Low water level	30°C, Unwelded Low water level	30°C, Welded High water level	30°C, Unwelded High water level	90°C, Welded, Low water level	90°C, Unwelded Low water level	90°C, Welded High water level	90°C, Unwelded High water level	
3	0.409	0.455	0.147	0.064	0.401	0.386	0.566	0.239	
	0.401	0.292	0.104	0.061	0.386	0.333	0.340	0.226	
	0.366	0.239	0.102	0.038	0.330	0.325	0.328	0.198	
	0.315	0.224	0.099	0.036	0.282	0.318	0.312	0.188	
	0.274	0.221	0.086	0.033	0.274	0.292	0.302	0.178	
	0.246	0.218	0.086	0.033	0.249	0.251	0.178	0.175	
	0.208	0.201	0.084	0.028	0.249	0.246	0.163	0.173	
	0.203	0.185	0.061	0.028	0.221	0.234	0.170	0.170	
	6	0.272	0.556	0.224	0.305	0.620	0.572	0.671	0.305
		0.269	0.381	0.208	0.239	0.584	0.521	0.422	0.287
0.257		0.358	0.203	0.193	0.434	0.495	0.401	0.277	
0.251		0.457	0.198	0.191	0.386	0.417	0.401	0.259	
0.239		0.439	0.193	0.183	0.378	0.411	0.366	0.218	
0.231		0.343	0.188	0.170	0.279	0.356	0.361	0.208	
0.216		0.335	0.178	0.165	0.236	0.330	0.356	0.191	
0.213		0.310	0.168	0.157	0.234	0.320	0.315	0.173	
12		0.483	0.521	0.455	0.404	0.544	0.996	0.841	0.645
		0.442	0.442	0.371	0.389	0.533	0.960	0.818	0.559
	0.409	0.429	0.361	0.386	0.493	0.871	0.732	0.518	
	0.404	0.419	0.343	0.381	0.483	0.843	0.620	0.462	
	0.394	0.409	0.328	0.366	0.460	0.831	0.610	0.462	
	0.381	0.401	0.323	0.361	0.445	0.813	0.574	0.457	
	0.368	0.391	0.282	0.310	0.378	0.798	0.569	0.442	
	0.368	0.391	0.254	0.295	0.371	0.785	0.569	0.439	

TABLE 6. (cont'd)

Exposure, months	30°C, Welded Low water level	30°C, Unwelded Low water level	30°C, Welded High water level	30°C, Unwelded High water level	90°C, Welded, Low water level	90°C, Unwelded Low water level	90°C, Welded High water level	90°C, Unwelded High water level	
18	0.406	0.503	0.328	0.531	1.712	1.229	1.036	0.599	
	0.312	0.485	0.325	0.381	0.973	1.031	0.686	0.536	
	0.305	0.472	0.320	0.356	0.963	0.953	0.630	0.500	
	0.295	0.467	0.300	0.358	0.912	0.841	0.536	0.483	
	0.290	0.378	0.246	0.282	0.871	0.691	0.533	0.465	
	0.262	0.376	0.229	0.282	0.833	0.602	0.498	0.445	
	0.163	0.315	0.221	0.272	0.734	0.538	0.478	0.422	
	0.163	0.274	0.216	0.262	0.597	0.465	0.452	0.409	
	24	0.653	0.671	0.599	0.366	1.765	0.978	0.655	0.772
		0.643	0.620	0.439	0.335	1.113	0.914	0.577	0.645
0.599		0.493	0.432	0.328	1.011	0.909	0.551	0.645	
0.569		0.467	0.363	0.249	1.003	0.838	0.546	0.599	
0.538		0.422	0.353	0.244	0.983	0.754	0.490	0.587	
0.193		0.401	0.320	0.234	0.965	0.747	0.465	0.584	
0.183		0.323	0.279	0.229	0.869	0.726	0.465	0.574	
0.170		0.302	0.264	0.224	0.820	0.696	0.462	0.508	
30		0.630	0.533	0.658	0.869	1.273	1.270	1.793	1.107
		0.533	0.490	0.650	0.805	1.176	1.212	1.600	0.998
	0.521	0.447	0.579	0.660	1.031	1.113	0.917	0.925	
	0.503	0.442	0.559	0.632	0.960	1.067	0.871	0.899	
	0.500	0.371	0.521	0.612	0.836	1.052	0.714	0.848	
	0.495	0.333	0.505	0.592	0.757	1.031	0.676	0.721	
	0.493	0.330	0.460	0.584	0.754	0.970	0.648	0.673	
	0.439	0.325	0.432	0.554	0.706	0.757	0.638	0.660	